Semi-empirical calculation of 12CH3D-H2 broadening coefficients and their temperature-dependence exponents for rovibrational lines in parallel bands

A.S. Dudaryonok, N.N. Lavrentieva, J. Buldyreva

▶ **To cite this version:**

A.S. Dudaryonok, N.N. Lavrentieva, J. Buldyreva. Semi-empirical calculation of 12CH3D-H2 broadening coefficients and their temperature-dependence exponents for rovibrational lines in parallel bands. Journal of Quantitative Spectroscopy and Radiative Transfer, 2019, 229, pp.157-165. 10.1016/j.jqsrt.2019.03.008 . hal-02736906

HAL Id: hal-02736906
https://hal.science/hal-02736906

Submitted on 22 Oct 2021

HAL is a multi-disciplinary open access archive for the deposit and dissemination of scientific research documents, whether they are published or not. The documents may come from teaching and research institutions in France or abroad, or from public or private research centers.

L'archive ouverte pluridisciplinaire **HAL**, est destinée au dépôt et à la diffusion de documents scientifiques de niveau recherche, publiés ou non, émanant des établissements d'enseignement et de recherche français ou étrangers, des laboratoires publics ou privés.

Distributed under a Creative Commons Attribution - NonCommercial 4.0 International License

Version of Record: https://www.sciencedirect.com/science/article/pii/S0022407319300871
Manuscript_ac7e3ecee99aaf7e8ff529448b915020

Semi-empirical calculation of $^{12}CH_3D$-H_2 broadening coefficients and their temperature-dependence exponents for rovibrational lines in parallel bands

A.S. Dudaryonok[a], N.N. Lavrentieva[a], J. Buldyreva[b,*]

[a] *V.E. Zuev Institute of Atmospheric Optics, Siberian Branch of the Russian Academy of Sciences, 1 Akademishian Zuev square, 634021 Tomsk, Russia*

[b] *Institut UTINAM, UMR 6213 CNRS, Université Bourgogne Franche-Comté, 16 Route de Gray, 25030 Besançon cedex, France*

Number of Figures: 6
Number of Tables: 2

* Corresponding author. Fax: +33 (0)3 81 66 64 75
E-mail address: jeanna.buldyreva@univ-fcomte.fr

Keywords:

Monodeuterated methane; H_2-broadening coefficients; temperature exponents; semi-empirical calculation; planetary atmosphere

© 2019 published by Elsevier. This manuscript is made available under the CC BY NC user license
https://creativecommons.org/licenses/by-nc/4.0/

Abstract

Hydrogen-broadening coefficients and their temperature-dependence exponents for $^{12}CH_3D$ (J, K) lines in the parallel ($\Delta K = 0$) ν_3 band are computed by a semi-empirical method employing analytical Anderson-type expressions with a few-parameter correction factor introduced to account for various deviations from Anderson's theory approximations. On the basis of experimentally observed J-dependences of line widths, this correction factor is taken in the traditional two-parameter form, and the parameters are determined from fits on some room-temperature measurements. After validation by comparison with available experimental data, the calculations are done for extended ranges of rotational quantum numbers ($0 \le J \le 70$, $0 \le K \le 20$) typically requested for spectroscopic databases. To get the temperature-dependence exponents, computations with the room-temperature parameters' values are repeated for various temperatures in the room-temperature containing range 200–400 K recommended for HITRAN and least-squares fit procedures are applied. Detailed P-Q-R-line lists are provided. With negligible vibrational dependence of CH_3D line widths, these data can be also employed for other A_1-type bands.

1. Introduction

Methane CH_4 and its monodeuterated isotopologue CH_3D are known to play a key role in the atmospheres of outer planets and their moons. Precise knowledge of spectroscopic parameters of these species is requested for reliable interpretation of atmospheric spectra, and in particular for radiative transfer analysis and global climate modeling. Spectral line positions, intensities, pressure-broadening and -shifting coefficients with their temperature dependences are necessary primarily for perturbation by main atmospheric constituents: nitrogen, hydrogen and helium (see, e.g., [1–4]).

Despite a low abundance of about $5x10^{-4}$, CH_3D absorbs relatively strongly in the transparency windows of CH_4, so that e.g. its $3\nu_2$ band was proposed as alternative to the ν_2 and ν_6 bands for outer-planet atmosphere searches [5]. For the self-broadening case, line intensities and positions in the triad $\nu_3/\nu_5/\nu_6$ were analyzed by Tarrago et al. [6] to get CH_3D rotational constants for the vibrational states ν_3=1, ν_5=1 and ν_6=1. Self-broadening and self-shift coefficients in the ν_2 band were measured by Predoi-Cross et al. [7].

The case of perturbation by H_2 has received less attention of experimentalists: a very limited number of measurements on CH_3D-H_2 line-broadening and line-shifting parameters were published. The ν_2 band located near 4.7 μm (P(5,2), P(7,2), P(7,3), P(8,3) lines) was investigated by Chudamani and Varanasi [8] in the temperature interval 94–300 K. Voigt-profile (VP) model was employed to deduce the broadening coefficients, and the associated temperature-dependence exponents were determined. VP-broadening coefficients at 131, 228, 295 K and their temperature dependences for two lines P(4,2,E) and P(5,3,A) in the fundamental ν_3 band (at 7.6 μm) were obtained by the same authors later [9]. The ν_3 band at room temperature was extensively studied by Lerot and collaborators [10] who tested Voigt, Rautian and Galatry profiles to extract broadening coefficients of 36 P- and R-lines ($1 \le J \le 15$, $0 \le K \le 9$). Owing to additional low-temperature experiments (153.5, 183.5 and 223.5 K), the authors obtained also [11] the temperature-dependence exponents corresponding to three abovementioned profiles for P(7,4,E), R(1,0,A+), R(3,2,E) and R(7,5,E) lines. For the fundamental ν_6 band (at 8.6μm) first broadening coefficients were measured at 296 K with VP-model for the transitions ^{R}P(5,2,E), ^{R}P(7,2,E), ^{P}P(11,2,E), ^{P}P(12,3,A-) and ^{P}P(12,5,E) [12]. For the same band, ^{P}P(6,1,E), ^{R}P(5,0,A+), ^{P}P(5,1,E) and ^{P}P(4,2,E) VP-line widths with temperature exponents were reported in the abovementioned paper [9]. Both broadening and shifting of room-temperature CH_3D-H_2 lines were studied in detail for the $3\nu_2$ band [13] which is of particular interest in planetology. A multispectrum fitting technique allowed determination of line-shape parameters for 221 transitions in the P-, Q- and R-branches ($0 \le K \le 6$ and $J \le 14$, $J \le 13$ and $J \le 12$, respectively). Comparing P-line broadening coefficients for the ν_2, ν_3, ν_6 and $3\nu_2$ bands, the authors concluded also about the negligible vibrational dependence in the A1-type bands.

First theoretical estimates of CH_3D lines by H_2 were communicated by Tejwani and Fox [14] who used the semi-classical Anderson theory and represented the intermolecular interactions by the

long-range terms including the dipole and octupole moments of CH_3D and the quadrupole moment of H_2. For the pure rotational band at 300 K they provided line widths for $J = 0–15$ and $K = 0$ as well as the corresponding temperature exponents (averaged over K) for the temperature interval 100–300 K. Their results were found to be about 30% too high with respect to measurements [12]. Lerot and coauthors [10] attempted an improved semi-classical approach with added hexadecapole moments of both colliders and interactions between each atom of the "linear" CH_3D molecule with each atom of H_2. Still overestimated for high J values and underestimated for $J \geq 3$ and $K \approx J$ theoretical line widths were obtained. Performing similar calculations for low temperatures, the authors deduced also theoretical temperature exponents for 4 lines studied experimentally [11]. Recently, a semi-classical approach with long- and short-range interactions of CH_3D considered as a symmetric top and exact classical trajectories was suggested [15]. Line-broadening coefficients and their temperature-dependence exponents for the range 200–300 K were computed for P-, Q- and R-lines ($0 \leq J \leq 20$, $0 \leq K \leq 20$) in parallel bands. Whereas for small K-values the calculated J-dependences of line widths compared very favorably with measurements in the ν_3 [10] and $3\nu_2$ [13] bands, for $K \geq 7$ the theoretical results were too low. The temperature exponents demonstrated a rapid decreasing with increasing J, contrary to nearly constant value of 0.5 issued from the Anderson theory [14].

The aim of the present work is to benefit from the advantages of the semi-empirical method to improve the agreement with available experimental room-temperature line widths for middle and high K-values. Once this agreement achieved, the obtained model parameters can be employed to compute the broadening coefficients in enlarged with respect to the experimentally accessible intervals of J (up to 70). Moreover, reasonable extrapolations of model parameters for higher than the measured K-values (up to 20) enable creating line-lists for the (J,K) sets requested by spectroscopic databases. Finally, with the help of additional computations at lower and higher temperatures to cover the room-temperature containing range 200–400 K indicated as one of ranges of interest in the HITRAN2016 edition [16], the temperature-dependence exponents can be extracted too. These theoretical results will complete the extremely scarce experimental data published in the literature on broadening and shifting of CH_3D lines by hydrogen pressure. They are expected to be useful for astronomers and planetary scientists interested in studies and modeling of the atmospheres of major planets and their satellites where CH_3D molecule has been detected.

The following section summarizes the salient features of the semi-empirical approach and comments on the determination of the model parameters and their extrapolation for high K. The comparison with the available room-temperature measurements is presented and discussed in Section 3. Section 4 is devoted to the temperature dependence of the calculated broadening coefficients. Concluding remarks are given in the final section.

2. Theoretical background

The semi-empirical (SE) method [17] employs a specific form of the semi-classical (SC) line-width and line-shift expressions [18] factorized into the transition strengths (generally well known for isolated active molecules) and the « efficiency functions » for the scattering channels (containing the influence of the interactions potential and much more difficult to be evaluated). The efficiency functions are further written as analytical Anderson-theory functions multiplied by correction factors for various *l*-th rank multipole moments of the active molecule. The role of these correction factors is to account for the real trajectory curvature, vibrational effects and corrections to the scattering matrix. For colliders with a clearly leading electrostatic interaction a single correction factor is sufficient: $l = 1$ (dipole) for the water vapor molecule, $l = 2$ (quadrupole) for the carbon dioxide molecule, etc. The particular mathematical form and the number of empirically adjustable parameters are chosen on the basis of experimentally observed dependence of line widths on the rotational quantum number *J*. For H_2O line widths smoothly decreasing with increasing *J* a two-parameter form works well [17], but for self-perturbed CH_3Cl and CH_3CN line widths characterized for small *K* by a local minimum on the *J*-dependences a more complex four-parameter expression becomes necessary [19,20]. It is noteworthy that the mathematical forms are chosen for their convenience and their ability to describe the measured line widths; no specific physical meaning is expected from the values and the number of fitted model parameters. Typically, some experimental room-temperature line widths (for low, middle and high *J*) are selected in the R-branch, and the correction factor parameters are adjusted on these experimental values. These parameters, being generally temperature- and branch-independent, allow further massive computations of broadening coefficients for thousands of lines in all branches and sub-branches for a minimal CPU cost. In such a way, additional low- and high-temperature calculations can be performed to get also, via a least-mean-squares fit procedure, the temperature-dependence exponents for creating complete line-lists.

The SE collisional line half-width γ_{if} for the optical transition $i \to f$ in the spectroscopically active molecule reads [17]

$$\gamma_{if} = A(i,f) + \sum_{l,i'} D^2(ii'|l) P_l(\omega_{ii'}) + \sum_{l,f'} D^2(ff'|l) P_l(\omega_{ff'}), \qquad (1)$$

where the summations of the products $D^2(..|l)P_l(...)$ of the transition strengths (reduced matrix elements) $D(ii'|l)$, $D(ff'|l)$ and the efficiency functions $P_l(\omega_{ii'})$, $P_l(\omega_{ff'})$ are made over the active-molecule multipole-moment ranks l and possible scattering channels $i \to i'$, $f \to f'$. The efficiency functions $P_l(\omega)$, as mentioned above, are written as the products of the analytical functions $P_l^A\omega)$ of the Anderson theory and the correction factors $C_l(\omega)$:

$$P_l(\omega) = P_l^A(\omega) C_l(\omega). \qquad (2)$$

The first term in the right-hand side of Eq. (1)

$$A(i,f) = \frac{n_b}{c} \sum_{J_2} \rho_{J_2} \int_0^\infty \mathrm{d}v v f(v) b_0^2(v, J_2, i, f) \tag{3}$$

comes from the cut-off procedure of the Anderson theory and depends on the numerical density of bath molecules n_b, their rotational populations in the ground vibrational state ρ_{J_2}, relative molecular velocities v following the Maxwell-Boltzmann distribution f(v) and the cut-off radius b_0; the division by the speed of light c is performed to get the widths in wave number units (cm^{-1}).

For the purposes of the present work the CH_3D-H_2 interaction potential was built as a sum of the electrostatic dipole-quadrupole and octupole-quadrupole interactions as well as the induction, dispersion and short-range terms. The used values of the multipole moments, mean polarizabilities and anisotropies for two colliding molecules are those given in Table 1 of Ref. [15].

To fit the model parameters we chose some experimental R-line widths in the ν_3 band (the most studied from the viewpoint of line-broadening coefficients) [10]. The molecular rotational constants were taken as $A_0 = 5.2502$ cm^{-1}, $B_0 = 3.8800$ cm^{-1} [7] for the ground state and $A_3 = 5.27409$ cm^{-1}, $B_3 = 3.8584$ cm^{-1} [6] for the vibrationally excited ν_3 state of the active molecule, and $B_0 = 59.33451$ cm^{-1} [21] for the linear perturbing molecule (supposed to be in its ground state).

Because of the leading dipole-quadrupole interaction, the usual two-parameter correction factor

$$C_1(\omega_{JJ'}) = \frac{c_1}{1 + c_2\sqrt{J}} \tag{4}$$

was assumed. The sets (c_1,c_2) were fitted for each experimentally observed K (K = 0–7) and extrapolated, on the basis of K = 0–7 trend, for higher $K \le 20$ (**Table 1**). The model parameters determined for the R-branch were used without any modification for line widths in the P- and Q-branches.

Table 1. Semi-empirical fitting parameters deduced from experimental values of room-temperature R-branch CH_3D-H_2 broadening coefficients [10] for $K \le 7$ and extrapolated, on the basis of experimental trends, for higher K. Uncertainties given in the last line correspond to the mean values for experimentally observed $5 \le K \le 7$.

K	c_1	c_2
0	1.00(3)	0.006(1)
1	0.90(4)	0.007(1)
2	0.80(5)	0.009(2)
3	1.35(9)	0.025(4)
4	2.60(4)	0.060(2)
5–20	2.8+0.2K (3)	0.02K (2)

3. Room-temperature broadening coefficients

Comparisons of SE-calculated room-temperature CH_3D-H_2 broadening coefficients with the measurements in the ν_3 band [10] (R- and P-branches) and in the $3\nu_2$ band [13] (P-, Q- and R-branches) are shown in Figs 1–3.[1] The SC computations from Refs [10, 15] are also added for completeness. The semi-empirical values are plotted solely up to $J = 20$ in order to see in detail the region where previous measurements and calculations are available.

Figure 1 illustrates the R-branch case. The SE results based on fitting to measurements provide naturally much better agreement with experimental data than the previously published semi-classical values *ab initio* calculated from model interaction potentials. For $K = 0,1$ all theoretical line widths are close to each other; a slightly smaller slope of SE J-dependences, matching better the experimental points, is observed with respect to the recent SC computations [15]. For higher K the under-estimation of broadening at low J stated in the semi-classical computations [15] is completely removed in the frame of the SE method. The slopes of the SE and SC curves are nearly identical, indicating a realistic picturing of short-range forces (responsible for large energy-gap transitions) in both approaches.

Figure 2 presents our semi-empirical results compared to measurements and semi-classical calculations for P-branch lines. The experimental values for the $3\nu_2$ band have large error bars and a quite pronounced dispersion because of the strong blending of the P-lines for $J > 10$ and difficulties to perform reliable fits [13]. Whereas the SC results [15] clearly underestimate the broadening for small J-values at K near and above four, the SE values compare very favorably with the measured line widths. This agreement with measurements justifies *a posteriori* the use of the SE model parameters deduced from R-branch line widths for calculations in the P-branch.

The case of Q-branch lines is shown in Fig. 3. As for the P-branch lines, line-mixing effects are very pronounced for some transitions, and large uncertainties and irregular behavior in J-dependences appear for the corresponding experimental points. Also from the experimental point of view, instead of smooth decreasing of broadening with increasing J observed in the R- and P-branches, for $K \geq 4$ at small J-values the measurements exhibit a clear maximum whose position shifts gradually to higher J with increasing K. Similar features have been observed on R- and P-lines in the CH_3D-N_2 $\nu_3/\nu_5/\nu_6$ triad ([22,23] and references therein). The semi-empirical calculations, similarly to Figs 1 and 2, demonstrate regular decreasing of broadening with increasing J, and this fact is easily understood from the use of the same values for model parameters. In consequence, for small K (≤ 3) the experimental trends are quite well reproduced but not the local maxima seen on the experimental curves for $K = 4$–6. Since the existence of these maxima is not yet confirmed by other measurements, we did neither change the mathematical form of the SE correction factor nor refit the (c_1,c_2) sets.

[1] The experimental data for the ν_2 band [8] are disregarded in our comparison since they nearly coincide with the results of Boussin et al. [13] for the $3\nu_2$ band and are published without uncertainties.

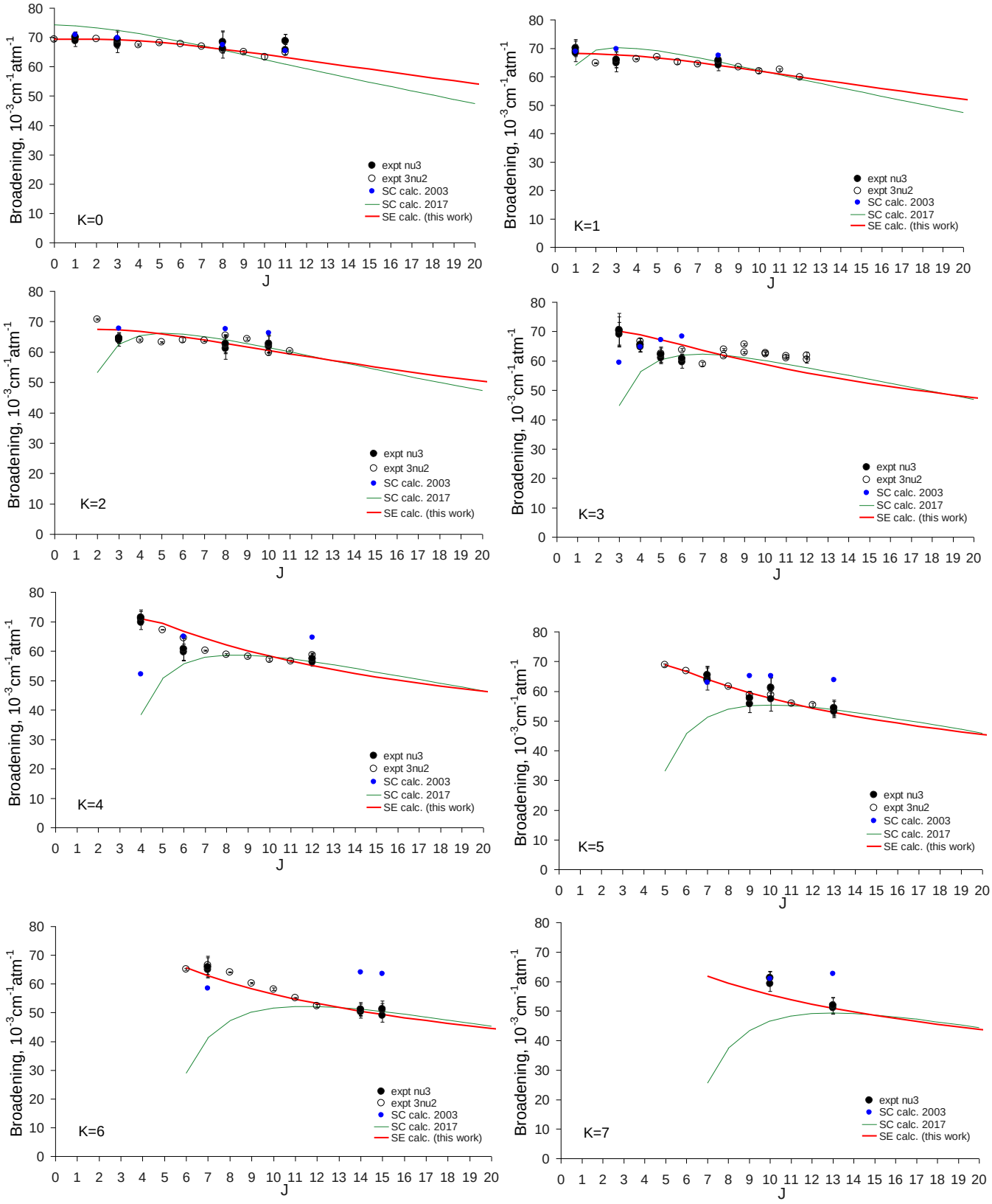

Figure 1. Comparison of experimental [10] and theoretical (semi-classical SC [10,15] and semi-empirical SE) *J*-dependences of room-temperature CH_3D-H_2 broadening coefficients at various *K* values for the R-branch of the ν_3 band. Voigt-, Rautian-, and Galatry-profile-values of Lerot et al. [10] are represented by the same symbols. The measurements of Boussin et al. [13] for the $3\nu_2$ band are also shown with identical symbols for the doublet lines.

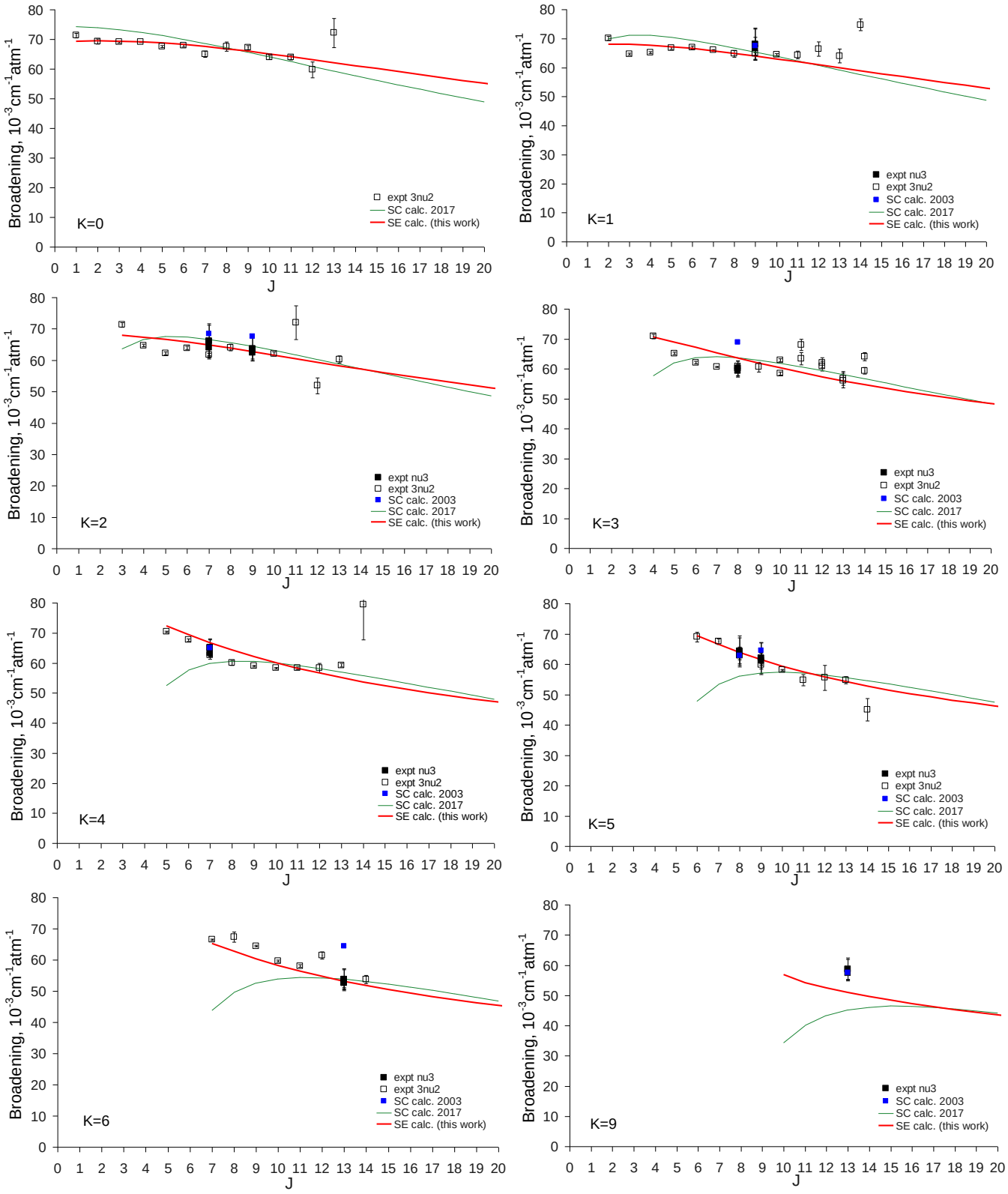
Broadening, 10^{-3}cm^{-1}atm^{-1}
J
K=0
K=1
K=2
K=3
K=4
K=5
K=6
K=9
expt nu3
expt 3nu2
SC calc. 2003
SC calc. 2017
SE calc. (this work)

Figure 2. Comparison of experimental [10] and theoretical (semi-classical SC [10,15]) and semi-empirical SE) *J*-dependences of room-temperature CH_3D-H_2 broadening coefficients at various *K* values for the P-branch of the ν_3 band. Voigt-, Rautian-, and Galatry-profile-values of Lerot et al. [10] are represented by the same symbols. The measurements of Boussin et al. [13] for the $3\nu_2$ band are also shown with identical symbols for the doublet lines.

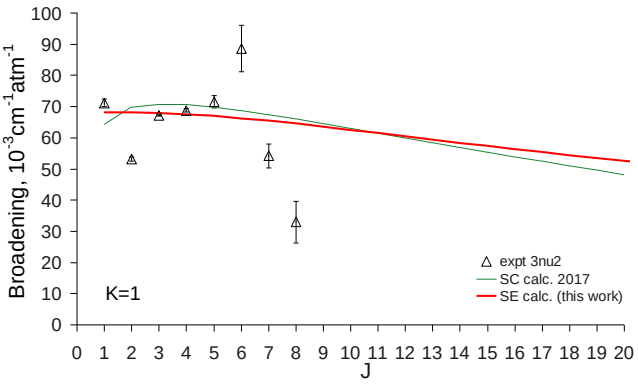
Broadening, 10^{-3}cm^{-1}atm^{-1}
J
K=1
expt 3nu2
SC calc. 2017
SE calc. (this work)

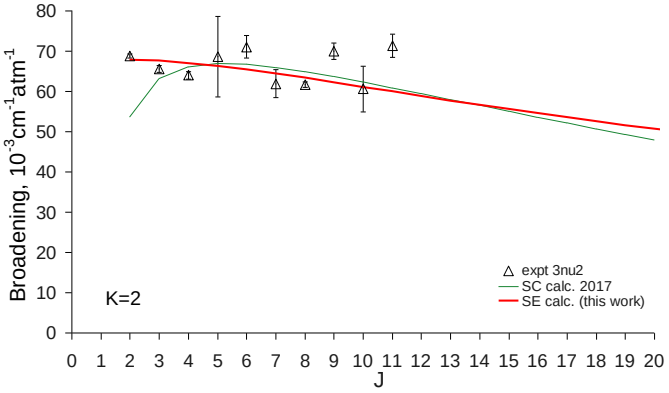
Broadening, 10^{-3}cm^{-1}atm^{-1}
J
K=2
expt 3nu2
SC calc. 2017
SE calc. (this work)

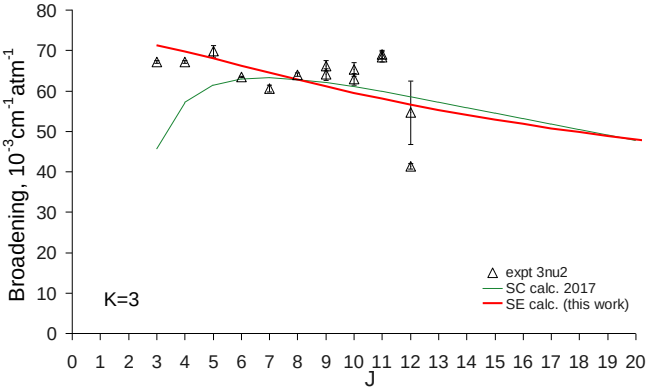
Broadening, 10^{-3}cm^{-1}atm^{-1}
J
K=3
expt 3nu2
SC calc. 2017
SE calc. (this work)

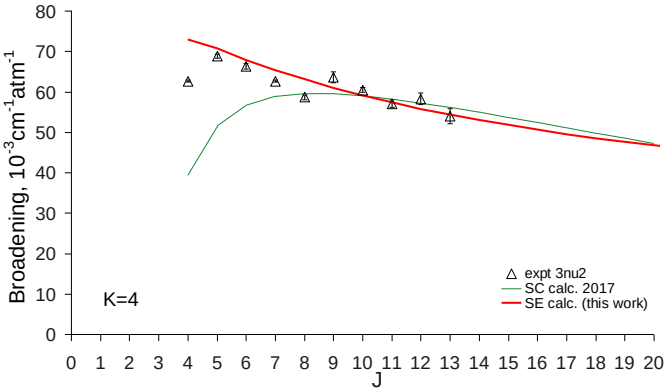
Broadening, 10^{-3}cm^{-1}atm^{-1}
J
K=4
expt 3nu2
SC calc. 2017
SE calc. (this work)

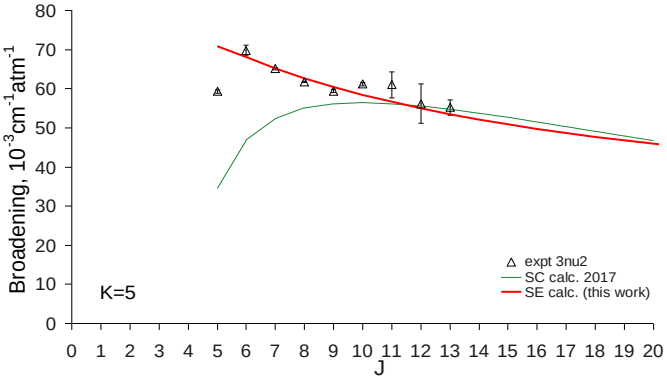
Broadening, 10^{-3}cm^{-1}atm^{-1}
J
K=5
expt 3nu2
SC calc. 2017
SE calc. (this work)

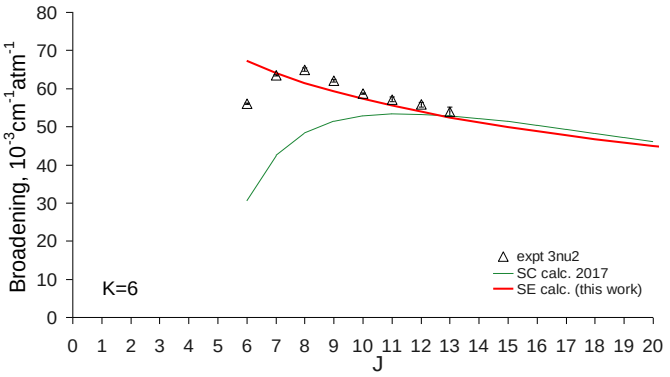
Broadening, 10^{-3}cm^{-1}atm^{-1}
J
K=6
expt 3nu2
SC calc. 2017
SE calc. (this work)

Figure 3. Comparison of theoretical *J*-dependences of room-temperature CH_3D-H_2 broadening coefficients calculated in [15] (SC) and in the present work (SE) at various *K* values for the Q-branch of the ν_3 band and experimental values obtained by Boussin et al. [13] for the $3\nu_2$ band.

To show the general trends of J-dependences after the experimentally probed region $0 \le J \le 15$, the full set ($0 \le J \le 70$, $K \le 20$) of SE-computed room-temperature line-broadening coefficients for the R-branch lines is plotted in Fig. 4.[2] The semi-classical results of Ref. [15] ($0 \le J \le 20$, $K \le J$) are also shown to underline the crucial difference between the J-dependences predicted by two approaches for small-J regions. The SE numerical values can be found in Supplementary material. Table 2 gives some examples for P-Q-R-lines with $K = 0$, 5 and $J \le 20$. As can be seen from this table comparing the lines with the same absolute value of the rotational quantum number m[3], for both $K = 0$ and $K = 5$ the branch-dependence of broadening coefficients is practically negligible: for P- and R-transitions the line-widths are identical, and for Q-transitions they are a little bit smaller.

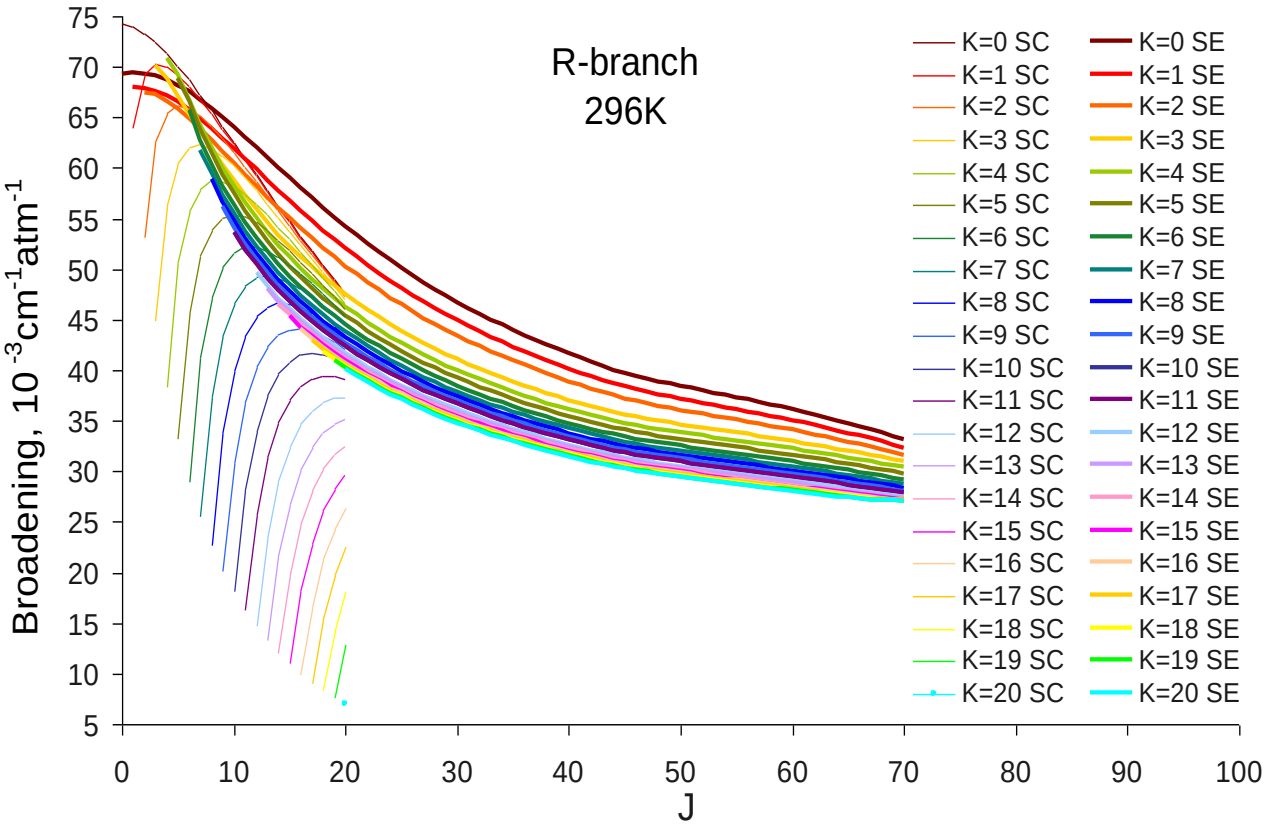

Figure 4. J-dependences of semi-empirical (SE) CH_3D-H_2 room-temperature broadening coefficients calculated at various fixed K for the R-branch of the ν_3 band. The semi-classical (SC) results [15] are shown for comparison.

[2] The sets corresponding to P- and Q-branches have very similar general behaviors and are not shown.
[3] $m = -J$ for the P-branch, $m = J$ for the Q-branch and $m = J + 1$ for the R-branch.

Table 2. Example of SE-calculated CH_3D-H_2 broadening coefficients γ (in $cm^{-1}atm^{-1}$) for K = 0 and 5 at the reference temperature of 296 K and corresponding temperature exponents N. J and K stand for the initial values of the rotational quantum numbers. The quoted uncertainties correspond to one standard deviation.

		P-branch				Q-branch				R-branch	
J	K	γ(296)	N	J	K	γ(296)	N	J	K	γ(296)	N
0	0			0	0			0	0	0.06936	0.619(11)
1	0	0.06937	0.619(15)	1	0	0.06940	0.619(16)	1	0	0.06940	0.620(16)
2	0	0.06940	0.620(16)	2	0	0.06939	0.621(16)	2	0	0.06932	0.621(16)
3	0	0.06933	0.621(16)	3	0	0.06926	0.622(16)	3	0	0.06911	0.622(17)
4	0	0.06911	0.622(17)	4	0	0.06897	0.622(17)	4	0	0.06874	0.621(17)
5	0	0.06874	0.621(17)	5	0	0.06852	0.621(18)	5	0	0.06823	0.619(18)
6	0	0.06822	0.619(18)	6	0	0.06793	0.618(18)	6	0	0.06757	0.616(18)
7	0	0.06757	0.616(18)	7	0	0.06721	0.615(19)	7	0	0.06681	0.613(19)
8	0	0.06681	0.613(19)	8	0	0.06640	0.611(19)	8	0	0.06596	0.609(19)
9	0	0.06596	0.609(19)	9	0	0.06551	0.607(19)	9	0	0.06504	0.605(19)
10	0	0.06504	0.605(19)	10	0	0.06456	0.602(20)	10	0	0.06409	0.600(20)
11	0	0.06409	0.600(20)	11	0	0.06359	0.598(20)	11	0	0.06310	0.596(20)
12	0	0.06310	0.596(20)	12	0	0.06260	0.593(20)	12	0	0.06211	0.591(20)
13	0	0.06210	0.591(20)	13	0	0.06159	0.589(20)	13	0	0.06110	0.587(20)
14	0	0.06110	0.587(20)	14	0	0.06059	0.585(20)	14	0	0.06010	0.582(19)
15	0	0.06010	0.582(19)	15	0	0.05959	0.581(19)	15	0	0.05912	0.579(18)
16	0	0.05912	0.579(18)	16	0	0.05856	0.577(19)	16	0	0.05809	0.575(19)
17	0	0.05809	0.575(19)	17	0	0.05753	0.573(19)	17	0	0.05709	0.572(19)
18	0	0.05709	0.572(19)	18	0	0.05654	0.570(19)	18	0	0.05611	0.569(18)
19	0	0.05611	0.569(18)	19	0	0.05557	0.568(18)	19	0	0.05515	0.566(17)
20	0	0.05515	0.566(17)	20	0	0.05463	0.565(16)	20	0	0.05422	0.563(16)
5	5			5	5	0.07072	0.620(16)	5	5	0.06890	0.619(17)
6	5	0.06949	0.619(18)	6	5	0.06798	0.618(17)	6	5	0.06662	0.617(18)
7	5	0.06662	0.617(19)	7	5	0.06512	0.616(18)	7	5	0.06391	0.615(18)
8	5	0.06391	0.615(18)	8	5	0.06259	0.614(18)	8	5	0.06152	0.613(18)
9	5	0.06152	0.613(18)	9	5	0.06037	0.611(19)	9	5	0.05941	0.610(18)
10	5	0.05941	0.610(18)	10	5	0.05838	0.608(19)	10	5	0.05751	0.607(19)
11	5	0.05751	0.607(19)	11	5	0.05658	0.605(18)	11	5	0.05579	0.604(18)
12	5	0.05579	0.604(18)	12	5	0.05495	0.602(18)	12	5	0.05423	0.600(17)
13	5	0.05423	0.600(17)	13	5	0.05346	0.598(17)	13	5	0.05280	0.597(17)
14	5	0.05280	0.597(17)	14	5	0.05211	0.595(17)	14	5	0.05151	0.594(17)
15	5	0.05151	0.594(17)	15	5	0.05087	0.593(17)	15	5	0.05031	0.592(17)
16	5	0.05031	0.592(17)	16	5	0.04972	0.590(17)	16	5	0.04920	0.589(17)
17	5	0.04920	0.589(17)	17	5	0.04864	0.587(17)	17	5	0.04815	0.586(16)
18	5	0.04815	0.586(16)	18	5	0.04764	0.585(16)	18	5	0.04718	0.584(16)
19	5	0.04718	0.584(16)	19	5	0.04670	0.582(15)	19	5	0.04628	0.581(15)
20	5	0.04628	0.581(15)	20	5	0.04583	0.580(14)	20	5	0.04544	0.579(15)

4. Temperature exponents

To obtain the temperature-dependence of CH_3D-H_2 broadening coefficients, the SE line widths were additionally computed for various temperatures from 200 to 400 K by the step of 50 K. Assuming that the line widths at temperature T obey the standard relation

$$\gamma(T) = \gamma(T_{ref})\left(\frac{T}{T_{ref}}\right)^{-N}, \quad (5)$$

the temperature exponents N were deduced for each (J,K) line by least-squares fits in log-log scale. The numerical values can be found in Supplementary material. Examples for the transitions with K = 0, 5 are given in Table 2.

Figure 5 shows the results obtained for the R-lines.[4] For this branch three experimental points (each with three profile models) and the corresponding semi-classical values are available [11]. The calculations of Tejwani and Fox [14] (averaged over K) and the SC values [15] are also of interest for comparison. Like the situation with the broadening coefficients, a striking difference is observed between the trends for the SE and the SC values of Ref. [15]. Because of the under-estimated at low J SC broadening coefficients the corresponding temperature exponents decrease very rapidly with increasing J. The SE values, due to their "Anderson-theory basis", demonstrate rather constant behavior similar to that of the Anderson-type data of Tejwani and Fox [14]. The similarity of these two series of results is additionally stressed by the very slight K-dependence of the semi-empirical curves. There is however a difference: the temperature exponents of Ref. [14] fluctuate around 0.5 whereas our SE calculations do it nearly around 0.6. This 0.6 value is still far from the estimate of the well-known resonance term of the Anderson theory [24] $N^A_{res} = 0.5 + (n-1)^{-1} \approx 0.83$ with $n = 4$ for the dipole-quadrupole interactions, but can be explained by the very small dipole moment of CH_3D. Indeed, the next non zero multipole for CH_3D is octupole ($n = 6$ for the octupole-quadrupole interactions), and N^A_{res} becomes equal to 0.7, i.e. close to our 0.6 value. The SE temperature exponents are also higher that the semi-classical computations of Lerot and coauthors [11] but are still inside the error bars of their measurements for K = 0 and 5. Other experimental studies of CH_3D-H_2 temperature exponents, especially for big values of rotational quantum numbers, would be extremely worthy to check the validity of our present calculations for all considered J and K.

[4] The lines P(4,2,E) and P(7,4,E) line studied, respectively, experimentally in [9] and experimentally and theoretically in [11] do not change our conclusions on comparison of our calculations with other data from the literature for the R-branch.

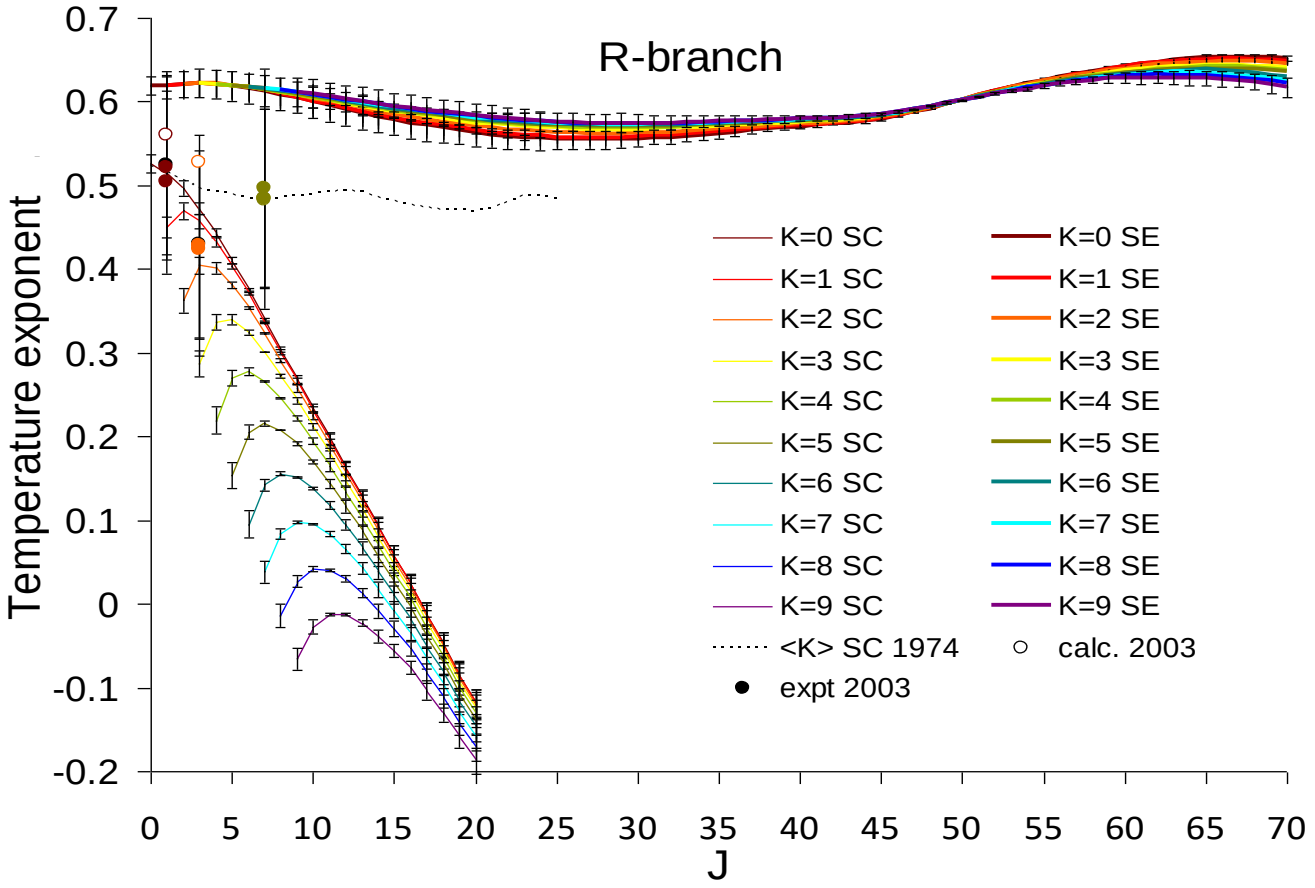

Figure 5. *J*-dependences of semi-empirical (SE) CH_3D-H_2 temperature exponents calculated in the present work for the *R*-branch of the ν_3 band (color solid lines with 1SD uncertainties shown) compared to the semi-classical (SC) results [15], to the averaged over $K = 0 – 10$ theoretical values of Tejwani and Fox [14] for the pure rotational band (dashed black line) as well as to calculations (color open circles) and measurements (color filled circles) of Lerot et al. [11] for 3 lines of the ν_3 band (experimental values deduced with Voigt, Rautian and Galatry profiles are represented by the same symbols).

Like Ref. [15], to test the semi-empirical temperature exponents we calculated the broadening coefficients for the R(1,0), R(3,2) and R(7,5) lines in the ν_3 band and compared them to the measurements [11] at 153.5, 183.5, 223.5 and 297 K (Fig. 6). For the sake of clarity we did not plot the previously published theoretical results. It is seen that for all three lines the good agreement of SE computations with measurements at room temperature becomes worse (overestimation respectively by 3.5%, 9.7% and 5.8% with respect to the experimental Rautian-profile values) for 223.5 K. At 183.5 and 153.5 K the overestimation is enhanced and reaches e.g. nearly 20% for the R(3,2) line. The disagreement at very low temperatures can be explained by the fact that the semi-empirical temperature exponents were evaluated for the temperature interval 200–400 K. Even at 223 K pertaining to this interval the semi-empirical (semi-classical by their nature) calculations seem to approach their limit of validity: the classical-trajectory notion becomes questionable and the "quantum-mechanical" character of the H_2 molecule brings additional difficulties. Again, new measurements for a big number of lines and at various temperatures would be of key importance to check the reliability of our calculations. Such measurements would allow in particular, checking the temperature-independence of the SE model parameters c_1, c_2 assumed, by analogy with the other previously studied molecular systems, for the CH_3D-H_2 case.

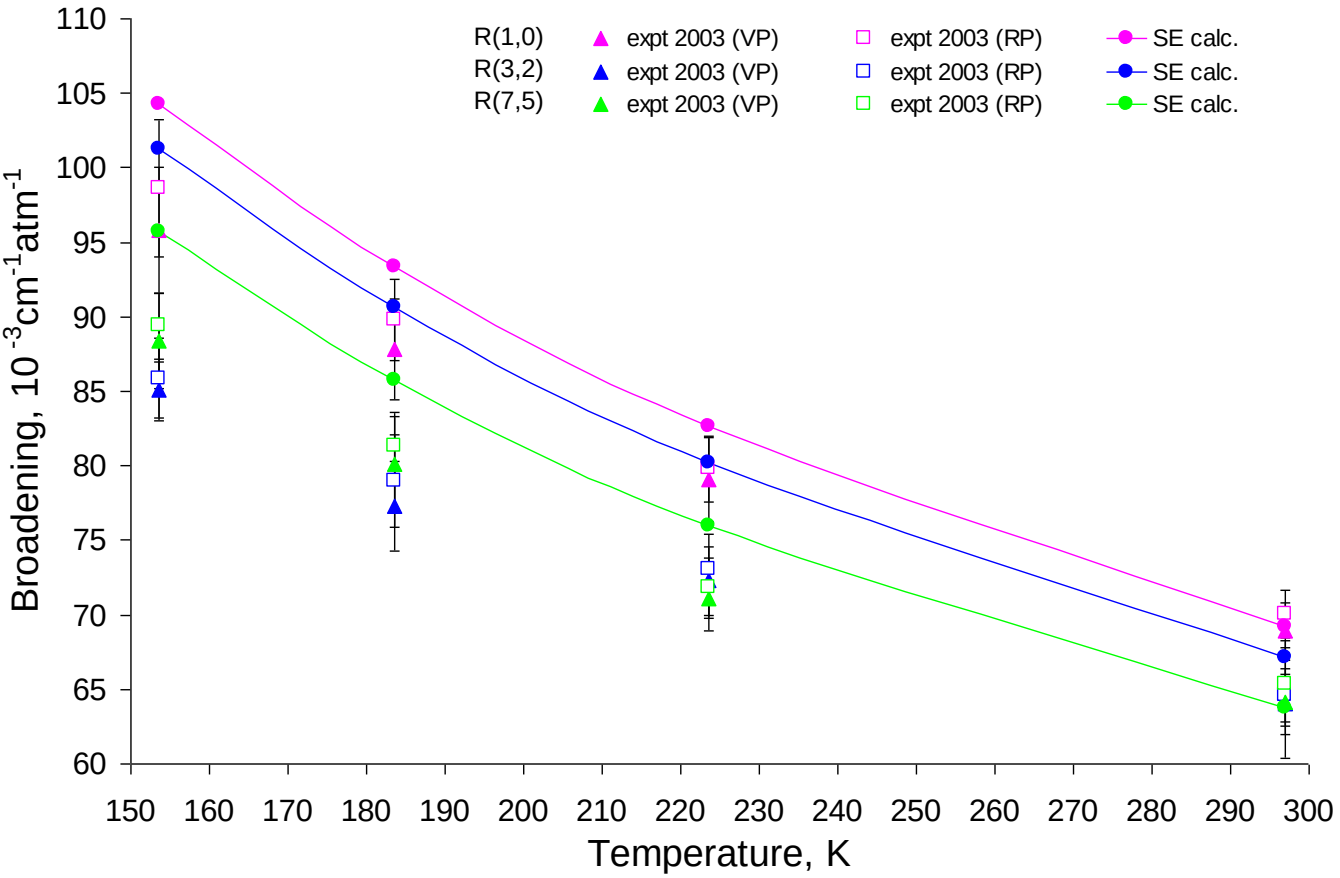

Figure 6. H_2-broadening coefficients restored for the CH_3D ν_3 lines $R(1,0)$, $R(3,2)$ and $R(7,5)$ with our semi-empirically (SE) calculated $\gamma(296)$ and N values in the temperature interval 150–300 K (solid lines with filled color circles). The experimental values [11] deduced with Voigt profile (VP) and Rautian profile (RP) are represented by color filled triangles and open squares, respectively. Other theoretical results from the literature are not shown for the sake of clarity.

5. Conclusion

We computed by a semi-empirical approach CH_3D-H_2 broadening coefficients and associated temperature-dependence exponents to be used in the temperature range 200–400 K for a large number of lines ($0 \le J \le 70$, $0 \le K \le 20$) in the R-, P- and Q-branches of the fundamental ν_3 band. Giving significantly better agreement with available room-temperature line-width measurements than the recently published semi-classical values, these results are expected to be more realistic estimates for the high-J transitions which have not been observed by the experimentalists. Even obtained for the parallel ν_3 band, our values can be used for other A_1-type bands (ν_2, $3\nu_2$, etc.) since a negligible vibrational dependence of line widths has been demonstrated experimentally by Boussin and collaborators. Our data can of interest for spectroscopic databases and studies of planetary atmospheres with quite high abundances of hydrogen and monodeuterated methane.

Acknowledgements

This work has been supported by the LIA SAMIA (*Laboratoire International Associé "Spectroscopie d'Absorption de Molécules d'Intérêt Atmosphérique et planétologique: de l'innovation instrumentale à la modélisation globales et aux bases de données"*) and by the Russian Foundation of Fundamental Research (grant n°17-52-16022).

Appendix A. Supplementary material

Supplementary data associated with this article can be found in the online version at http://...

References

[1] Fletcher LN, Orton GS, Teanby NA, Irwin PGJ, Bjoraker GL. Methane and its isotopologues on Saturn from Cassini/CIRS observations. Icarus 2009;199:351–67.

[2] Kuroda T, Medvedev AS, Hartogh P. Parameterization of radiative heating and cooling rtaes in the atmosphere of Jupiter. Icarus 2014;242:149–57.

[3] Irwin PGJ, de Bergh C, Courtin R, Bézard B, Teanby NA, Davis GR, Fletcher LN, Orton GS, Calcutt SB, Tice D, Hurley J. The application of new methane line absorption data to Gemini-N/NIFS and KPNO/FTS observations of Uranus' near-infrared spectrum. Icarus 2012;220:369–82.

[4] Maltagliati L, Bézard B, Vinatier S, Hedman MM, Lellouch E, Nicholson PD, Sotin C, de Kok RJ, Sicardy B. Titan's atmosphere as observed by Cassini/VIMS solar occultations: CH_4, CO and evidence for C_2H_6 absorption. Icarus 2015;248:1–24.

[5] Lutz BL, de Bergh C, Maillard JP. Monodeuterated methane in the outer solar system. I Spectroscopic analysis of the bands at 1.55 and 1.95 microns. Astrophys J 1983 ;273:397–409.

[6] Tarrago G, Delaveau M, Fusina L, Guelachvili G. Absorption of $^{12}CH_3D$ at 6–10 μm: Triad ν_3, ν_5, ν_6. J Mol Spectrosc 1987;126:149–158.

[7] Predoi-Cross A, Hambrook K, Brawley-Tremblay M, Bouanich J-P, Devi VM, Benner DC, Brown LR. Measurements and theoretical calculations of self-broadening and self-shift coefficients in the ν_2 band of CH_3D. J Mol Spectrosc 2005;234:53–74.

[8] Chudamani S, Varanasi P. Measurements on 4.7 μm CH_3D lines broadened by H_2 and N_2 at temperatures relevant to planetary atmospheres. JQSRT 1987;38:179–81.

[9] Varanasi P, Chudamani S. Linewidth measurements in the thermal infrared bands of $^{12}CH_3D$ at planetary atmospheric temperatures. Appl Op. 1989;28:2119–22.

[10] Lerot C, Walrand J, Blanquet G, Bouanich J-P, Lepere M. Diode-laser measurements and calculations of H_2-broadening coefficients in the ν_3 band of CH_3D. J Mol Spectrosc 2003;217:79–86.

[11] Lerot C, Walrand J, Blanquet G, Bouanich J-P, Lepere M. H_2-broadening coefficients in the ν_3 band of CH_3D at low temperatures. J Mol Spectrosc 2003;219:329–334.

[12] Lacome N, Cappellani F, Restelli G. Tunable diode laser measurements of broadening coefficients of lines in the ν_6 fundamental of $^{12}CH_3D$. Appl Opt 1987;26:766–768.

[13] Boussin C, Lutz BL, Hamdouni A, de Bergh C. Pressure broadening and shift coefficients for H_2, He and N_2 in the $3\nu_2$ band of $^{12}CH_3D$ retrieved by a multispectrum fitting technique. JQSRT 1999;63:49–84.

[14] Tejwani GDT, Fox K. Calculated self- and foreign-gas-broadened linewidths for CH_3D. J Chem Phys 1974;61:759–62.

[15] assical H_2-broadening coefficients of $^{12}CH_3D$ rovibrational

lines and their temperature dependence for planetary atmosphere modeling. Icarus 2017;282C:363–74.

[16] Gordon IE, Rothman LS, Hill C, Kochanov RV, Tan Y, Bernath PF, et al. The HITRAN2016 molecular spectroscopic database. JQSRT 2017;203:3–69.

[17] Bykov AD, Lavrentieva NN, Sinitsa LN. Semiempiric approach for the line broadening and shifting calculation. Mol Phys 2004;102:1653–8.

[18] Robert D, Bonamy J. Short range force effects in semiclassical molecular line broadening calculations. J Phys 1979;40:923–43.

[19] Dudaryonok AS, Lavrentieva NN, Buldyreva J. CH_3Cl self-broadening coefficients and their temperature dependences. JQSRT 2013;130:321–6.

[20] Dudaryonok AS, Lavrentieva NN, Buldyreva JV. CH_3CN self-broadening coefficients and their temperature dependences for the Earth and Titan atmospheres. Icarus 2015;250: 76–82.

[21] Bragg SL, Brault JW, Smith WH. Line positions and strengths in the H_2 quadrupole spectrum. Astrophys J 1982;263:999–1004.

[22] Predoi-Cross A, Devi MV, Sung K, Sinyakova T, Buldyreva J, Benner DC, Smith MAH, Mantz A. Temperature dependences of N_2-broadneing and shift coefficients in the ν_6 perpendicular band of CH_3D. JQSRT 2015;163:120–41.

[23] Predoi-Cross A, Devi MV, Sutradhar P, Sinyakova T, Buldyreva J, Sung K, Smith MAH, Mantz A. Temperature dependences of self- and N_2-broadened line-shape parameters in the ν_3 and ν_5 bands of $^{12}CH_3D$: Measurements and calculations. JQSRT 2016;177:181–215.

[24] Birnbaum G. Microwave pressure broadening and its application to intermolecular forces. Adv Chem Phys 1967;12:487–548.